Please cite this article in press as: Bögershausen et al., Recessive *TRAPPC11* Mutations Cause a Disease Spectrum of Limb Girdle Muscular Dystrophy and Myopathy with ..., The American Journal of Human Genetics (2013), http://dx.doi.org/10.1016/j.ajhg.2013.05.028

REPORT

Recessive *TRAPPC11* Mutations Cause a Disease Spectrum of Limb Girdle Muscular Dystrophy and Myopathy with Movement Disorder and Intellectual Disability

Nina Bögershausen,[1,2,3,19] Nassim Shahrzad,[4,19] Jessica X. Chong,[5,19] Jürgen-Christoph von Kleist-Retzow,[6] Daniela Stanga,[4] Yun Li,[1,2,3] Francois P. Bernier,[7,10] Catrina M. Loucks,[7] Radu Wirth,[1] Eric G. Puffenberger,[8] Robert A. Hegele,[9] Julia Schreml,[1,2,3] Gabriel Lapointe,[4] Katharina Keupp,[1,2,3] Christopher L. Brett,[4] Rebecca Anderson,[5] Andreas Hahn,[11] A. Micheil Innes,[7,10] Oksana Suchowersky,[12] Marilyn B. Mets,[13] Gudrun Nürnberg,[14] D. Ross McLeod,[7] Holger Thiele,[14] Darrel Waggoner,[5] Janine Altmüller,[14] Kym M. Boycott,[15] Benedikt Schoser,[16] Peter Nürnberg,[2,3,14] Carole Ober,[5,17] Raoul Heller,[1] Jillian S. Parboosingh,[7,10] Bernd Wollnik,[1,2,3,*] Michael Sacher,[4,18,*] and Ryan E. Lamont[7,19]

Myopathies are a clinically and etiologically heterogeneous group of disorders that can range from limb girdle muscular dystrophy (LGMD) to syndromic forms with associated features including intellectual disability. Here, we report the identification of mutations in transport protein particle complex 11 (*TRAPPC11*) in three individuals of a consanguineous Syrian family presenting with LGMD and in five individuals of Hutterite descent presenting with myopathy, infantile hyperkinetic movements, ataxia, and intellectual disability. By using a combination of whole-exome or genome sequencing with homozygosity mapping, we identified the homozygous c.2938G>A (p.Gly980Arg) missense mutation within the gryzun domain of TRAPPC11 in the Syrian LGMD family and the homozygous c.1287+5G>A splice-site mutation resulting in a 58 amino acid in-frame deletion (p.Ala372_Ser429del) in the foie gras domain of TRAPPC11 in the Hutterite families. *TRAPPC11* encodes a component of the multiprotein TRAPP complex involved in membrane trafficking. We demonstrate that both mutations impair the binding ability of TRAPPC11 to other TRAPP complex components and disrupt the Golgi apparatus architecture. Marker trafficking experiments for the p.Ala372_Ser429del deletion indicated normal ER-to-Golgi trafficking but dramatically delayed exit from the Golgi to the cell surface. Moreover, we observed alterations of the lysosomal membrane glycoproteins lysosome-associated membrane protein 1 (LAMP1) and LAMP2 as a consequence of TRAPPC11 dysfunction supporting a defect in the transport of secretory proteins as the underlying pathomechanism.

Limb girdle muscular dystrophies (LGMDs) are a heterogeneous group of genetic myopathies leading primarily to proximal muscle weakness, with relative sparing of heart and bulbar muscles, except for some subtypes.[1,2] So far mutations at over 50 loci with either autosomal-dominant (LGMD1) or autosomal-recessive inheritance (LGMD2) have been described.[3] The major forms of LGMD result from mutations in genes encoding constituents of the sarcolemmal dystrophin complex, e.g., laminin (LGMD1B), sarcoglycan (LGMD2C-F), and dysferlin (LGMD2B). Other forms, however, result from mutations in genes affecting muscle function via different pathomechanisms involving membrane trafficking,[4] muscle remodeling,[5] and posttranslational modification of sarcolemmal proteins.[6] The age of onset, severity, and rate of progression vary considerably between LGMD subtypes, ranging from early childhood myopathy to adult onset with long-time preserved ambulation. The spectrum of dystroglycanopathies even ranges from mild LGMD to severe congenital muscular dystrophy with brain and eye involvement and severe intellectual disability (ID).[6] ID is defined as an intelligence quotient <70 and significant limitations in two or more adaptive skills identified in childhood[7] and is found in 1%–3% of the general population.[8] ID is etiologically heterogeneous with genetic and nongenetic causes and can be found as the sole clinical feature in nonsyndromic ID or as part of a syndrome with other clinical manifestations. Disruption of a number of cellular and embryological processes have been linked to ID such as transcriptional control of neuronal genes,

[1]Institute of Human Genetics, University Hospital Cologne, 50931 Cologne, Germany; [2]Center for Molecular Medicine Cologne (CMMC), University of Cologne, 50931 Cologne, Germany; [3]Cologne Excellence Cluster on Cellular Stress Responses in Aging-Associated Diseases (CECAD), University of Cologne, 50674 Cologne, Germany; [4]Department of Biology, Concordia University, Montreal, QC H4B 1R6, Canada; [5]Department of Human Genetics, University of Chicago, Chicago, IL 60637, USA; [6]Pediatrics Department, University Hospital Cologne, 50931 Cologne, Germany; [7]Department of Medical Genetics, University of Calgary, Calgary, AB T2N 4N1, Canada; [8]Clinic for Special Children, Strasburg, PA 17579, USA; [9]Robarts Research Institute and University of Western Ontario, London, ON N6G 2V4, Canada; [10]Alberta Children's Hospital Research Institute, University of Calgary, Calgary, AB T2N 4N1, Canada; [11]Department of Child Neurology, University Hospital Giessen, 35392 Giessen, Germany; [12]Departments of Medicine, Medical Genetics, and Psychiatry, University of Alberta, Edmonton, AB T6G 2B7, Canada; [13]Department of Ophthalmology, Lurie Children's Hospital of Chicago, Northwestern University, Chicago, IL 60611, USA; [14]Cologne Center for Genomics, University of Cologne, 50931 Cologne, Germany; [15]Children's Hospital of Eastern Ontario Research Institute, University of Ottawa, Ottawa, ON K1H 8L1, Canada; [16]Friedrich-Bauer-Institute, Ludwig-Maximilian-University Munich, 80336 Munich, Germany; [17]Department of Obstetrics, University of Chicago, Chicago, IL 60637, USA; [18]Department of Anatomy and Cell Biology, McGill University, Montreal, QC H3A 2B2, Canada
[19]These authors contributed equally to this work
*Correspondence: bwollnik@uni-koeln.de (B.W.), michael.sacher@concordia.ca (M.S.)
http://dx.doi.org/10.1016/j.ajhg.2013.05.028.

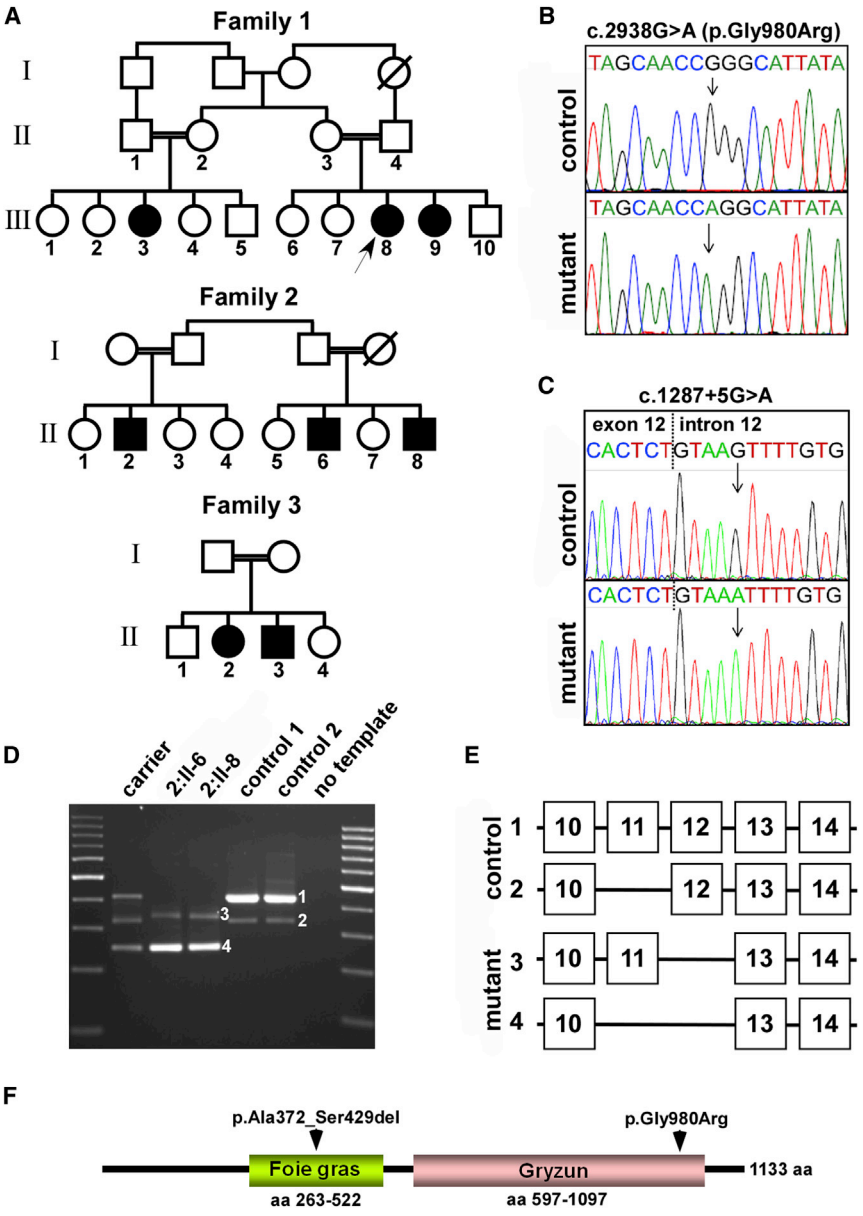

Figure 1. Pedigrees and Molecular Characterization of the *TRAPPC11* Mutations

(A) Pedigree structure of families 1, 2, and 3.

(B) Representative wild-type (WT) and mutant electropherograms from family 1. The c.2938G>A mutation is indicated by a black arrow.

(C) Representative WT and mutant electropherograms from families 2 and 3 demonstrating the homozygous c.1287+5G>A mutation (indicated by a black arrow) in relation to the exon 12 and intron 12 boundary.

(D) RT-PCR analysis confirmed the presence of altered C11 splicing in lymphocytes obtained from one carrier parent, two affected individuals, and two controls. Numbers 1, 2, 3, and 4 correspond to different transcripts illustrated in (E).

(E) Schematic representation of these RT-PCR products after gel isolation and Sanger sequencing. In control cells, the full-length transcript (1) predominates over an alternatively spliced minor transcript lacking exon 11 (2). In cells from affected individuals, the minor transcript lacks only exon 12 (3), whereas the predominant transcript (4) lacks both exons 11 and 12, resulting in an in-frame deletion of 58 amino acids (p.Ala372_Ser429del).

(F) Schematic representation of TRAPPC11 and the location of the foie gras and gryzun domains. The two mutations identified in this study are indicated by black arrows.

neuronal development and synapse formation, and intracellular signaling, as well as intracellular trafficking.[8,9] Here, we report on the clinical, molecular, and cellular phenotype of an autosomal-recessively inherited disease spectrum that ranges from LGMD to a syndrome characterized by myopathy, ID, hyperkinetic movements, and ataxia, resulting from altered vesicle trafficking.

The study was conducted on a consanguineous Syrian family with an uncharacterized form of LGMD (family 1; Figure 1A) and two families of Hutterite ancestry[10,11] (families 2 and 3; Figure 1A) with affected individuals presenting with a myopathic syndrome associated with moderate ID, infantile hyperkinetic movements, and ataxia. All subjects or their legal representatives gave written informed consent to the study and the research protocols were approved by the respective institutional review board. The study was performed in accordance with the Declaration of Helsinki protocols. Fibroblasts were cultivated from a skin biopsy from individual III-8 of family 1 and the two siblings (II-6 and II-8) from family 2 following standard protocols after written informed consent had been given.

The three affected individuals from family 1 were born to healthy first-cousin parents (Figures S1A–S1C). They suffer from a progressive proximal muscle weakness, with onset by early school age and 9- to 16-fold increased serum creatine kinase (CK) levels, that led to different degrees of impaired ambulation. The younger cousins are ambulatory with moderate limitations due to fatigue and muscle pain, whereas the eldest cousin (III-3), at age 26, has severely limited mobility (unable to climb stairs, walks short distances with much difficulty) reflecting the progressive nature of the disease. In all affected individuals, the shoulder girdle muscles are less severely involved than the hip girdle musculature. Skeletal findings, present in all affected individuals, include hip dysplasia and scoliosis. In addition, individual III-3 presented with a mild bilateral cataract and individual III-8 showed strabismus convergens. Except for a slight enlargement of the right cardiac ventricle in individual III-9, there was no obvious cardiac or bulbar muscle involvement (Table 1).

Please cite this article in press as: Bögershausen et al., Recessive *TRAPPC11* Mutations Cause a Disease Spectrum of Limb Girdle Muscular Dystrophy and Myopathy with ..., The American Journal of Human Genetics (2013), http://dx.doi.org/10.1016/j.ajhg.2013.05.028

Table 1. Clinical Features

	Family 1			Family 2			Family 3	
Individual	**III:8**	**III:9**	**III:3**	**II:2**	**II:6**	**II:8**	**II:2**	**II:3**
TRAPPC11 mutation	c.2938G>A p.Gly980Arg	c.2938G>A p.Gly980Arg	c.2938G>A p.Gly980Arg	c.1287+5G>A	c.1287+5G>A	c.1287+5G>A	c.1287+5G>A	c.1287+5G>A
Gender	female	female	female	male	male	male	female	male
Age (years)	20	16	26	25	22	20	20	18
Height (centile)	10^{th}	$25–50^{th}$	25^{th}	$<5^{th}$	3^{rd}	$<3^{rd}$	50^{th}	$5–10^{th}$
OFC (centile)	25^{th}	$50–75^{th}$	$10–25^{th}$	50^{th}	$<2^{nd}$	$<<<3^{rd}$	$<3^{rd}$	$<3^{rd}$
Muscular symptoms	prox. weakness, muscle pain, muscle cramps	prox. weakness, muscle pain, muscle cramps	prox. weakness, muscle pain	none	mild muscle weakness	none	none	Hypotonia in early childhood
Muscle biopsy	n/a	n/a	myopathic changes	myopathic changes	myopathic changes	n/a	n/a	n/a
CK levels (u/l)	~2,700	1,300–2,800	600–1,600	490–1,215	300–600	700–1,000	1,009	728
DTR	UE+/ LE−	UE+/ LE+	UE−/ LE−	UE+/ LE+	UE+/ LE+	UE+/ LE+	UE+/ LE+	UE+/ LE+
Heart	not involved	enlarged RV	not involved	not involved	not involved	not involved	not involved	not involved
Skeletal symptoms	hip dysplasia, scoliosis, no contractures	hip dysplasia, mild scoliosis, no contractures	hip dysplasia, scoliosis, no contractures	limb asymmetry	none	none	none	none
Intellectual disability	no	no	mild	mild to moderate	moderate	moderate	mild, IQ 60 (WISC-III)	mild, IQ 60 (TONI-3)
Development	motor delay	normal	unknown	global delay	global delay	global delay	global delay	global delay
Seizures	none	none	none	none	abnormal EEG	primary generalized	abnormal EEG	none
Ataxia	none	none	none	truncal	truncal	truncal	truncal	truncal
Choreiform movements	none	none	none	truncal and limb	truncal and limb	generalized	generalized	limb and facial
Neuroimaging (MRI)	n/a	n/a	n/a	normal	mild cerebral atrophy	mild cerebral atrophy	normal	normal
Ocular	esotropia, myopia	none	bilateral cataract, myopia	none	none	none	exophoria anisometropia, amblyopia	none

CK, creatine kinase; DTR, deep tendon reflexes; EEG, electroencephalogram; ID, intellectual disability; LE, lower extremity; MRI, magnetic resonance imaging; n/a, not applicable; OFC, occipital frontal circumference; Prox., proximal; RV, right ventricle; TONI-3, Test of Nonverbal Intelligence, Third Edition v3; UE, upper extremity; u/l, units/liter; WISC, Wechsler Intelligence Scale for Children; +, normal; −, absent.

Pulmonary function testing revealed a moderate restrictive respiratory disorder in individual III-3, while clinical signs of sleep disordered breathing could not be objectified by overnight oxymetry and capnography. The younger cousins do not yet show signs of respiratory involvement. Individual III-3 displayed mild ID.

We performed whole-exome sequencing on DNA extracted from blood lymphocytes of individual III-8. After enrichment of exonic sequences with the SureSelect Human All Exon 50 Mb kit (Agilent Technologies, Santa Clara, CA, USA), the exome was sequenced on an Illumina Genome Analyzer IIx Sequencer (Illumina, San Diego, CA, USA) with two lanes of a single-end 150 basepair protocol. Bioinformatic analysis of all exome variants was used to determine stretches of homozygosity. To refine the homozygous regions, we additionally performed genome-wide linkage analysis in the three affected individuals and their parents by using the Affymetrix GeneChip® Human Mapping 250K Array (Affymetrix, Santa Clara, CA, USA). Genotypes were called by the GeneChip® DNA Analysis Software (GDAS v2.0, Affymetrix) and analyzed as previously decribed.[12–16] Linkage analysis was performed assuming autosomal-recessive inheritance, full penetrance, consanguinity, and a causative variant frequency of 0.0001. A single linked homozygous region of 1.03 Mb on chromosome 4q35.1 (defined by SNPs rs6823077 and rs12502711; chr4: 183833940–184866656, hg19; Figures S1D and S1E) containing nine annotated genes was determined. The only unannotated variant in the exome data set within this critical region was the homozygous missense variant c.2938G>A (p.Gly980Arg; Figure 1B) in *TRAPPC11* (Table S1; RefSeq accession number NM_021942.5). *TRAPPC11* codes for a 1,133 amino acid protein containing a so-called foie gras and a gryzun domain (Figure 1F). The variant

affects a highly conserved amino acid residue within the gryzun domain (Figure 1F; Figure S1F) that is predicted to affect protein structure by PolyPhen-2. Cosegregation of the c.2938G>A variant within the family was confirmed by Sanger sequencing (data not shown). The mutation was not found in 100 healthy Turkish controls tested either by restriction enzyme digestion with the enzyme MvaI or direct Sanger sequencing and is not annotated in any current database of human variation including >12,000 alleles of the Exome Variant Server (Exome Variant Server, NHLBI GO Exome Sequencing Project [ESP], Seattle, WA). Furthermore, screening of all coding exons of *TRAPPC11* by Sanger sequencing in 32 German single cases of unclassified recessive LGMD did not identify an additional *TRAPPC11* mutation. Screening of the exome data of genes in which recessive mutations are known to cause LGMD did not identify a pathogenic mutation.

The Hutterites are an endogamous Anabaptist group that arose during the Protestant Reformation in South Tyrol and, upon arrival in North America during the 1870s, established three groups, the Dariusleut, Schmiedeleut, and Lehrerleut that have remained mostly genetically isolated from one another.[17] The Hutterite families in this study consisted of two affected brothers and their affected first cousin from the Dariusleut Hutterites of Alberta (family 2; Figure 1A; Figures S2A and S2B) and two affected siblings (one male, one female) from the Schmiedeleut Hutterites of South Dakota (family 3; Figure 1A; Figures S2C and S2D). An eight-generation pedigree connects the affected individuals to their most recent common Hutterite ancestors, a couple born in the 1790s (Figure S3), prior to the founding of the three leuts. All affected individuals from families 2 and 3 have a history of early onset developmental delay and as young adults now have mild to moderate ID. There is no history of regression, and neuroimaging was unremarkable; in particular, no abnormalities in the cerebellum or basal ganglia were observed. As young children, they all had significant evidence of a hyperkinetic movement disorder mainly characterized by choreiform movements of trunk, limbs, and head although athetoid movements, tremors, and dystonic posturing were also noted. In addition, all affected individuals had a truncal ataxia resulting in further gait instability (Table 1). Metabolic investigations including plasma, urine, and cerebrospinal fluid failed to identify any specific anomalies. Mild muscle weakness with persistently elevated CK levels suggested an associated myopathy. The two limb girdle muscular dystrophies known to be present in the Hutterite population, LGMD2H (MIM 254110; *TRIM32*, NM_012210.3, c.1459G>A; p.Asp487Asn)[18] and LGMD2I (MIM 607155; *FKRP*, NM_024301.4, c.826C>A; p.Leu276Ile)[19] were excluded in all five individuals by Sanger sequencing. Although the two families were not closely related, a founder mutation with an autosomal recessive mode of inheritance was suspected because of the Hutterites' history of genetic isolation.

Homozygosity mapping in the two affected siblings from family 2 and two of their unaffected siblings was performed by using a 10K SNP genotyping microarray (Affymetrix), and two relevant blocks of homozygosity on chromosomes 1p31.3 and 4q34.3-q35.1 were identified (Figure S2E). Haplotype analysis across the two regions including all three affected individuals from family 2 ruled out the region on chromosome 1p31.3 (data not shown). The remaining region on chromosome 4q34.3-q35.1 (flanked by the SNPs rs721684 and rs726466; chr4: 177850523–186546056, hg19) was 8.7 Mb in size and contained 47 predicted or known genes and 10 predicted or known noncoding RNAs (Table S2). Whole-exome sequencing was undertaken on a single affected individual from family 2 by using the SureSelect Human All Exon v2 kit (Agilent Technologies) and paired-end sequencing on an Illumina GAII (Illumina) performed commercially by Perkin Elmer (Branford, CT, USA). Reads were mapped to the reference sequence and variants were called by using the CLC genomics workbench (CLCbio, Cambridge, MA, USA). Within the single region of shared identity by descent, only three variants were not in dbSNP with a population frequency of less than 0.02. Only the c.1287+5G>A splice-site variant at the donor site of exon 12 of *TRAPPC11* (NM_021942.5; Figure 1C) was considered to be pathogenic. The variant was predicted to abolish the exon 12 splice donor site by in silico analysis by using the Alamut software (Interactive Software, San Diego, CA).

Family 3 was investigated by whole-genome sequencing (Complete Genomics, Mountain View, CA, USA) of both affected siblings and both parents. A total of 2,714 variants were heterozygous in both parents, homozygous in both affected siblings, and absent in the homozygous state in a database of 94 other Hutterite genomes. However, only eight of these were annotated as altering the protein-coding sequence or splicing of a gene. With the exception of *TRAPPC11* c.1287+5G>A, the same mutation identified in family 2, these remaining variants were common (minor allele frequency ≥10%) in the other Hutterite genomes or in dbSNP. *TRAPPC11* is located within a 1.69 Mb homozygous haplotype on chromosome 4q35.1 (chr4: 184562444–186254248, hg19) shared by both affected siblings in family 3. Segregation studies via Sanger sequencing of *TRAPPC11* c.1287+5G>A in both family 2 and 3 verified that all five affected individuals were homozygous for the variant, all parents were heterozygous, and all unaffected siblings carried one or no copies of the variant (data not shown).

The same c.1287+5G>A mutation identified in two separate Hutterite leuts in individuals with similar phenotypes substantiated the suspicion of a founder mutation present prior to the leut subdivision. Thus, we screened for this mutation in a normal control population of 1,827 individuals from all three Hutterite leuts by using a custom TaqMan genotyping assay (Applied Biosystems, Foster City, CA, USA) and did not identify any individuals

who were homozygous for the mutant allele, adding support for the pathogenicity of this mutation. We observed carrier frequencies of approximately 7% in both the Dariusleut and Schmiedeleut. The mutation was not detected in the Lehrerleut (Table S3). Given the carrier frequencies in the two leuts, we would expect approximately 1 in 750 individuals to be homozygous for this mutation, suggesting that this mutation might account for some of the unexplained syndromic forms of ID in the Hutterite population.

Because the *TRAPPC11* c.1287+5G>A mutation was predicted to alter splicing of the exon 12 donor site, we determined the effect on the mature *TRAPPC11* transcript by using RT-PCR followed by sequencing of the resulting fragments. In control lymphocytes, two splice isoforms were observed: the predominant splice isoform consists of the full-length transcript, whereas the minor splice isoform lacks exon 11 and is predicted to result in premature protein truncation (Figures 1D and 1E). In lymphocytes from affected individuals, the predominant splice isoform lacks both exons 11 and 12 resulting in a 58 amino acid in-frame deletion in the foie gras domain (p.Ala372_Ser429del), whereas the minor splice isoform lacks only exon 12 and is predicted to result in a prematurely truncated protein (Figures 1D and 1E). Multiple species alignment of TRAPPC11 using Multalin[17] demonstrated numerous amino acids within the deleted segment that are highly conserved (Figure S2F), suggesting that this region is important in protein function.

TRAPP (transport protein particle) is a multiprotein complex involved in ER-to-Golgi trafficking.[20] It was initially identified in *Saccharomyces cervisiae*[21] and is conserved across species.[22] The subunit TRAPPC11 (C11) is a TRAPP component that is important for complex integrity and anterograde membrane transport from the endoplasmic reticulum (ER) to the ER-to-Golgi intermediate compartment (ERGIC) in mammals.[22] It is ubiquitously expressed in humans, reflecting its important role in basic cellular functions. C11 participates in numerous interactions with other TRAPP complex components, most notably TRAPPC2 (C2), TRAPPC2L (C2L), TRAPPC6, TRAPPC10, and TRAPPC12.[22] Loss-of-function mutations in the zebrafish ortholog of C11 have been found in the *foie gras* mutant, characterized by steatohepatitis and eye development defects, respectively.[23,24] In Drosophila S2 cells, RNAi knockdown of C11 blocks Golgi exit.[25] In HeLa cells, small interfering RNA (siRNA) knockdown of C11 leads to impaired binding of other TRAPP components, functional impairment of the complex, retention of secretory proteins in the ERGIC, and fragmentation of the Golgi apparatus.[22,25]

Immunostaining of the Golgi apparatus with the marker protein GM130 (BD Biosciences, San Jose, CA, USA) was performed in primary fibroblasts from individual III-8 of family 1 and the two siblings from family 2, as well as on control cells. Punctate Golgi dispersal was observed in cells from affected individuals similar to that seen after TRAPPC11 knockdown in HeLa cells[22] (Figures 2A–2E). Quantitation of the fragmented phenotype indeed shows a higher percentage of cells with a fragmented Golgi in cells from affected individuals compared to controls (Figure 2F). The Golgi phenotype was confirmed by immunostaining for a second Golgi marker mannosidase II (manII; courtesy of Dr. Kelley Moremon) in family 2 (data not shown). Confocal microscopy of the Golgi in individual III-8 from family 1 further illustrated the scattered Golgi network (Figure 2G) and three-dimensional (3D) reconstruction of confocal microscopy images from family 2 confirmed that the fragmentation is due to fewer and/or thinner connections between the GM130-positive structures (Figures 2H and 2I).

Consistent with the punctate Golgi seen upon C11 knockdown, immunoblot analysis demonstrated a quantitative reduction of full-length mutant C11 protein in fibroblasts from families 1 and 2 (Figures 2J and 2K). In family 2, there is an accumulation of what might possibly be TRAPPC11 fragments due to their cross-reactivity with anti-TRAPPC11. If these fragments are indeed truncated polypeptides of TRAPPC11, they are incapable of interacting with TRAPPC2 (Figure 2L), suggesting that the instability of TRAPPC11 in these individuals might either cause or result from an inability to interact with TRAPP, a distinction that we cannot presently address. Similarly, although C11 p.Gly980Arg was unstable in cells derived from affected individuals, we exploited the stability of this protein in a yeast system to demonstrate that the protein loses its ability to interact with several TRAPP proteins by yeast two-hybrid analysis (Figure S4). An unrelated substitution in proximity to C11 p.Gly980Arg (C11 p.Trp986_Arg988delinsAlaGluAsp) also showed the same inability to interact with TRAPP proteins (Figure S4; Table S4) indicating that this region of C11 might be important for its interactions and stability.

In order to determine whether cells from affected individuals also displayed a block in membrane traffic between the endoplasmic reticulum (ER) and the Golgi, we used VSV-G-ts045-GFP (VSV-G) as a marker for transport along the secretory pathway. This commonly used marker protein misfolds at elevated temperatures (40°C) and is retained in the ER. Upon shifting to lower temperature (32°C) and in the presence of the protein synthesis inhibitor cycloheximide, the ER-restricted material exits and is transported to the Golgi and ultimately to the cell surface.[26] The kinetics of this transport is well documented with appearance of the protein in the Golgi within minutes of release, where it can reside for up to 40 minutes before transport to the cell surface.[27] We assessed VSV-G localization in fibroblasts from affected individuals from family 2 and control fibroblasts, in conjunction with the Golgi marker manII, at fixed intervals. The trafficking experiments were performed in cell lines from both affected individuals from family 2; however, data is shown only for individual II-8 for simplicity. After incubation at 40°C, VSV-G is found exclusively in the ER in both control

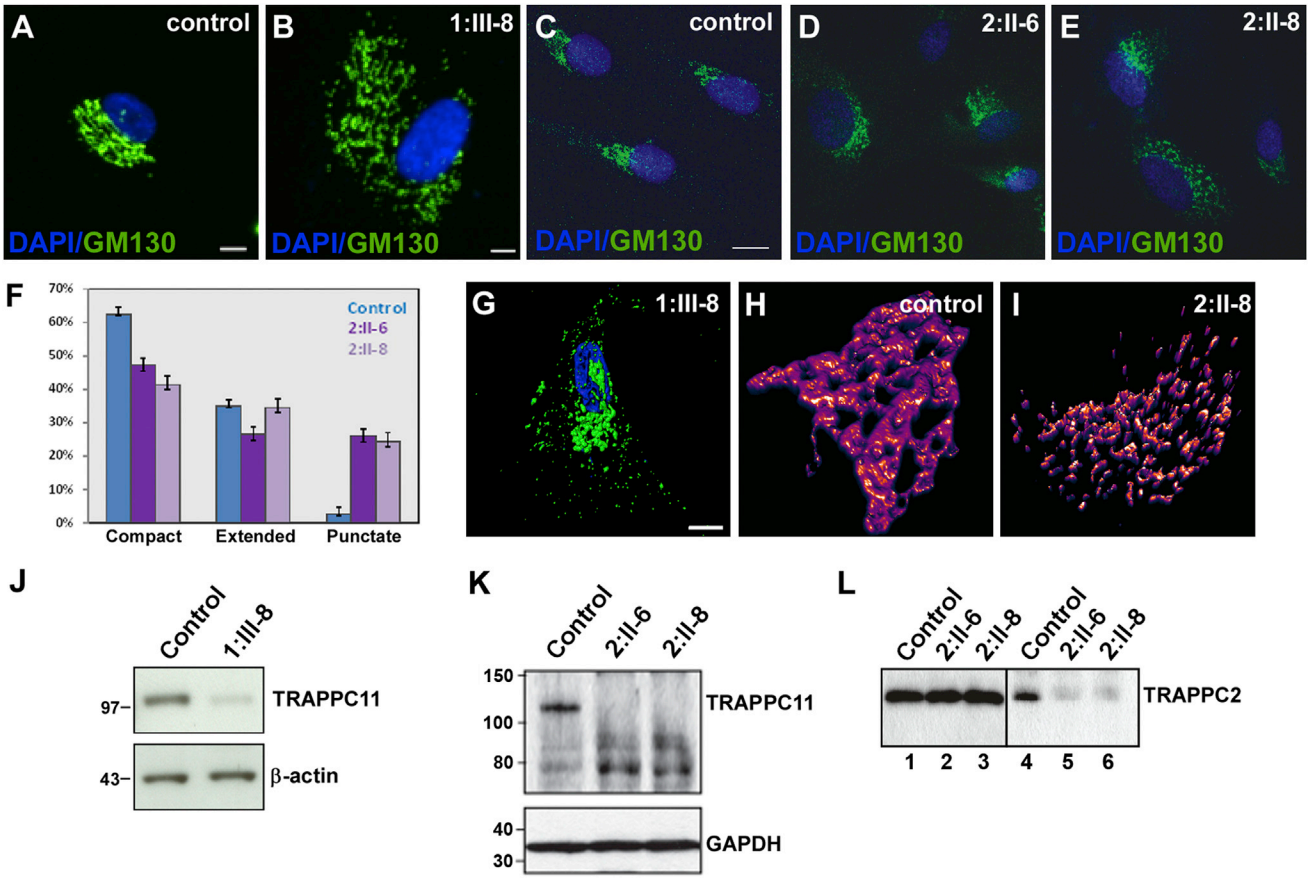

Figure 2. ***TRAPPC11*** **Mutations Alter Golgi Morphology, Protein Stability and TRAPP Assembly**
(A–E) Immunostaining of fibroblasts from affected individuals and controls with GM130 antibody and DAPI show that the affected individuals have disrupted Golgi morphology compared to healthy controls. Scale bars represent 10 μm.
(F) Quantitation of the Golgi phenotype seen in the cells from (C)–(E). A minimum of 300 cells for each sample were quantitated over three independent experiments.
(G) High-resolution confocal image of a fibroblast from individual III-8 of family 1 illustrating the scattered Golgi structure. The scale bar represents 10 μm.
(H and I) 3D reconstruction of a z stack of the Golgi from a control cell and from individual II-8 of family 2.
(J and K) Immunoblot analysis of cell lysates from individual 1:III-8 (J) or 2:II-6 and 2:II-8 (K) fibroblasts show a reduction of full-length C11 in comparison to control cells. Different mobility of C11 results from different types of gel and buffer used for the experiments shown in (J) and (K). Note the presence of possible C11 fragments in (K) suggesting a destabilization of the protein as a result of the c.1287+5G>A mutation.
(L) Lysates from fibroblasts from individuals II-6 and II-8 of family 2 (lanes 1–3) and control were prepared, and equal amounts (0.5 mg) were incubated with anti-C11 IgG. The immune complexes were collected onto beads (lanes 4–6), eluted, and probed for the TRAPP protein C2. Lanes 1–3 show equal amounts of C2 in the starting material. The C2 and C11 antibodies are noncommercial, generated by the group of M.S. in rabbits against full-length His-tagged C2 and a peptide derived from the carboxy-terminal region of C11. Antibodies were used as described.[22]

cells and cells from affected individuals, displaying the typical diffuse, reticular pattern (Figure 3A). Colocalization of VSV-G with the Golgi marker manII is clearly seen after 30 minutes following release from the ER at 32°C in both control cells and cells from affected individuals (Figure 3A). After 120 minutes, however, virtually all of the VSV-G is found on the cell surface of control cells while a significant amount of VSV-G remains in the Golgi of cells from affected individuals (Figure 3A). Live-cell imaging confirmed delayed VSV-G exit from the Golgi in cells from affected individuals, pronounced from approximately 90 minutes, consistent with the findings of the timed intervals above (Movie S1). The delay of VSV-G exit from the Golgi in cells from the affected individuals suggests that generalized trafficking of molecules through the Golgi might be delayed in these individuals as a result of the in-frame deletion of TRAPPC11.

Delayed exit from the Golgi could arise from a defect in anterograde traffic from the Golgi to the cell surface or indirectly from defects in the endocytic pathway that would fail to retrieve material from the Golgi needed for anterograde traffic. To determine whether the trafficking defect observed in cells from affected individuals was due to defects in the endocytic pathway, we examined the uptake of fluorescently tagged transferrin from the cell medium but did not observe any uptake defects

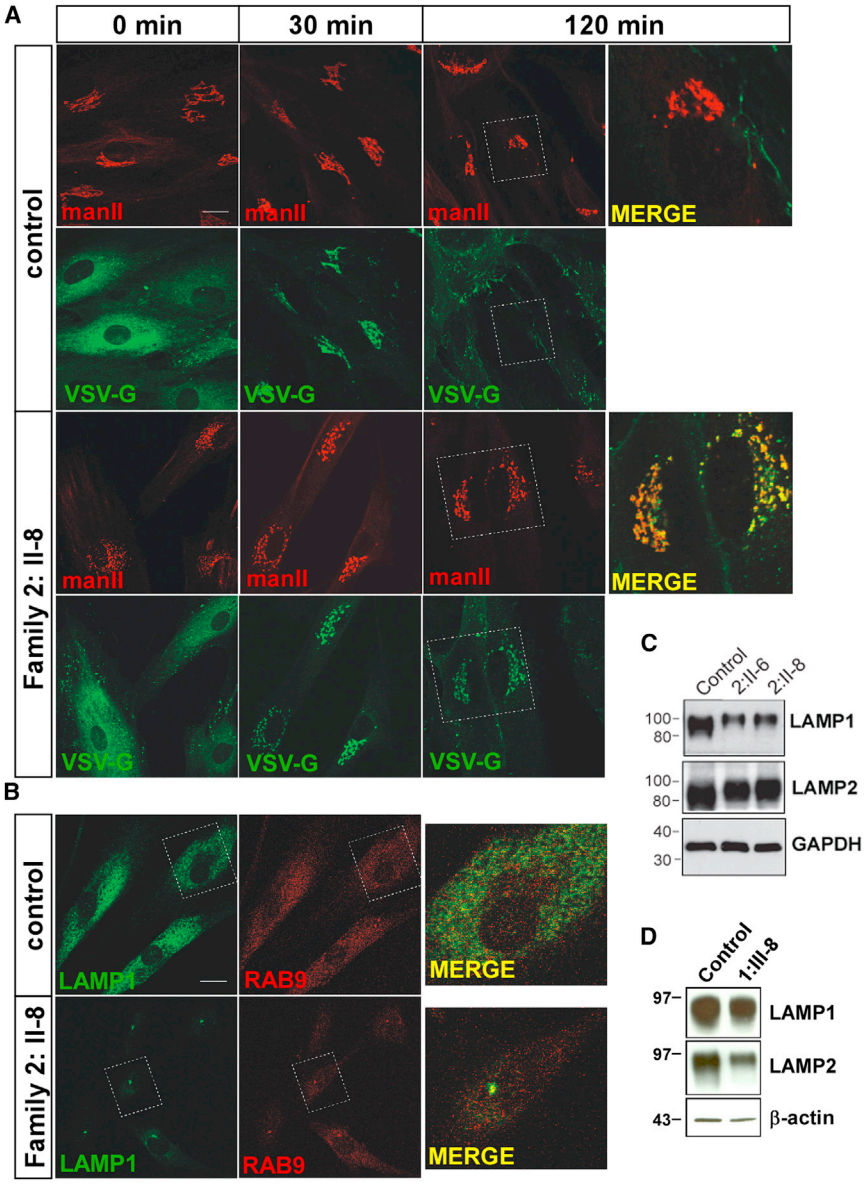

Figure 3. Altered VSV-G Trafficking and LAMP1 Localization in Cells from Affected Individuals

(A) Fibroblasts from a control and individual II:8 of family 2 were infected with virus expressing VSV-G-ts045-GFP (VSV-G) for 1 hr and then incubated overnight at 37°C. The cells were then shifted to 40°C for 6 hours at which point cyclohexamide was added and the samples were transferred to 32°C. Samples were removed at 0, 30, and 120 min following transfer to 32°C and stained with the Golgi marker mannosidase II (manII). The scale bar represents 10 μm.

(B) Immunostaining with the late endosome/lysosome markers Rab9 and LAMP1 (Abcam, Cambridge, UK) demonstrated a normal diffuse pattern of both proteins in control fibroblasts but strong perinuclear localization in cells from affected individuals. The scale bar represents 10 μm.

(C) Equal amounts of lysate prepared from control, individual II:6 and individual II:8 of family 2 were probed for LAMP1, LAMP2 (Abcam), and GAPDH as a loading control.

D) Equal amounts of cell lysate from fibroblasts of individual III:8 of family 1 and control fibroblasts were incubated with monoclonal antibodies against LAMP1, LAMP2 (H4A3 and H4B4, respectively; Santa Cruz Biotechnology, Santa Cruz, USA), and β-actin as a loading control.

(data not shown). However, immunostaining of cells from affected individuals from family 2 for the late endosomal/lysosomal component lysosome-associated membrane protein 1 (LAMP1) identified a striking difference in the localization pattern compared to control cells (Figure 3B). LAMP1 in control cells was seen in puncta throughout the cell with the occasional deposition in the perinuclear region (24% ± 1% of control cells [n = 189]), similar to other studies reporting LAMP1 localization.[28] Conversely, fibroblasts from affected individuals displayed prominent perinuclear staining for LAMP1 in a high proportion of cells (78% ± 2% and 87%±3% of cells in individual II-6 and individual II-8, respectively [n = 189 for all cases]). Immunostaining of cells from affected individuals from family 2, as well as immunoblotting of the corresponding cell lysates, showed a reduced level of LAMP1 compared to control (Figures 3B and 3C) and was concentrated in a higher molecular-size region than in the control, suggesting that it might be more highly glycosylated. Levels of lysosome associated membrane protein 2 (LAMP2) did not appear to be significantly reduced in cells from affected individuals from family 2 but, like LAMP1, the protein appeared to be more highly glycosylated (Figure 3C). Moreover, immunoblot analysis of fibroblasts from individual III-8 of family 1 also showed LAMP1 and LAMP2 alterations (Figure 3D).

Retention of the human growth-hormone marker protein GFP-F_M4-hGH in the Golgi of HeLa cells following knockdown of C11 was previously reported.[25] In addition, ablation of C11 by siRNA was reported to result in accumulation of VSV-G in a brefeldin A-resistant compartment, interpreted to be related to the ERGIC (ER-Golgi intermediate compartment).[22] Our finding that partial deletion of the foie gras domain of C11 leads to defects in a post-Golgi compartment might be explained by a milder functional effect of the p.Ala372_Ser429del deletion compared to knockdown of the entire protein. It is noteworthy that several recent studies implicated the TRAPP complex in retrograde traffic originating at the cell surface; however, the precise location where TRAPP acts in this pathway

was not addressed.[29,30] Our present study suggests that a C11-containing TRAPP complex is involved in the formation and/or movement of late endosomes/lysosomes. A prominent perinuclear staining of LAMP1 has been seen in cells depleted of Rab9, leading to the suggestion that effector molecules required for late endosomal transport are not recruited in the absence of this GTPase.[31] In addition, Rab7 and the lipid composition of membranes has been implicated in the motility of late endosomes/lysosomes.[32] It will be of interest in the future to examine the relationship between a C11-containing TRAPP complex and various GTPases involved in late endosome dynamics.

Mutations in *TRAPPC2* and *TRAPPC9*, encoding TRAPP complex components, cause X-linked spondyloepiphyseal dysplasia tarda[33] and postnatal microcephaly with ID,[34,35] respectively. It has been suggested that the different effects of mutations in *TRAPPC2* and *TRAPPC9* on human disease are linked to the specific function and binding capacities of each subunit.[36] The similar Golgi phenotype observed in fibroblasts from affected individuals from families 1 and 2 suggests similar functional effects of both *TRAPPC11* mutations on TRAPP composition and function. Phenotypic differences between our families could be explained by different functional consequences of each alteration, residing in different protein domains.

Our finding of LAMP1/LAMP2 alterations suggest a similarity with the pathomechanism of Danon disease (MIM 300257), a myopathy caused by LAMP2 deficiency,[37] characterized by dilatative cardiomyopathy, proximal skeletal muscle weakness, and ID.[38] Danon disease is a rare X-linked dominant disorder with early childhood onset and an aggressive disease course in male affected individuals, leading to death from cardiac complications in the 2nd to 3rd decade, if not prevented by heart transplantation. Female affected individuals show a milder disease course, but many suffer from mild ID and muscle weakness in addition to cardiac manifestations. Both sexes might develop retinopathy, hepatic, and pulmonary disease.[38,39] The molecular pathogenesis of Danon disease exemplifies that defects in intracellular trafficking components can cause a skeletal muscle phenotype with associated ID.

In summary, we present a form of autosomal-recessive, slowly progressive LGMD with childhood onset and high CK, as well as a syndrome consisting of myopathy, ID, hyperkinetic movements, and ataxia, caused by homozygous mutations in the membrane trafficking component *TRAPPC11*. Thus, the presence of myopathy and high CK with or without additional symptoms in a person should alert clinicians for TRAPPC11 deficiency. Both mutations lead to a range of molecular defects including altered TRAPP complex composition, impaired Golgi morphology, and altered protein transport along the secretory pathway. These results suggest that altered membrane trafficking is the underlying molecular mechanism of this disease spectrum.

Supplemental Data

Supplemental Data include four figures, four tables, and one movie and can be found with this article online at http://www.cell.com/AJHG.

Acknowledgements

We are grateful to all family members that participated in this study and to Karin Boss and Bob Argiropolous for critically reading the manuscript, Leo Dimnik for assistance with NGS data, and Kelley Moremon for the manII antibody. This work was supported by the German Federal Ministry of Education and Research (BMBF) by grant number 01GM1211A (E-RARE network CRANIRARE-2) to B.W., by the Canadian Institutes of Health Research and the Natural Sciences and Engineering Council of Canada to M.S., research grant #5-FY09-529 from the March of Dimes Foundation to K.M.B., and the National Institutes of Health grants R01HD21244 and R01HL085197 to C.O. R.E.L. was supported by a Remax clinical fellowship from the Alberta Children's Hospital Foundation and K.M.B. is supported by a Clinical Investigatorship Award from the Canadian Institutes of Health Research, Institute of Genetics. M.S. is a member of the Groupe de Recherche Axé sur la Structure des Protéines (GRASP) network.

Received: March 19, 2013
Revised: April 22, 2013
Accepted: May 28, 2013
Published: July 3, 2013

Web Resources

The URLs for the data presented herein are as follows:

NHLBI Exome Sequencing Project (ESP) Exome Variant Server, http://evs.gs.washington.edu/EVS/
GeneCards: http://www.genecards.org
MultAlin: http://multalin.toulouse.inra.fr/multalin/
National Center for Biotechnology Information, http://www.ncbi.nlm.nih.gov/
Online Mendelian Inheritance in Man (OMIM), http://www.omim.org/
PolyPhen-2, http://www.genetics.bwh.harvard.edu/pph2/
UCSC Genome Browser, http://genome.ucsc.edu
UniProt, http://www.uniprot.org/

References

1. Rosales, X.Q., and Tsao, C.Y. (2012). Childhood onset of limb-girdle muscular dystrophy. Pediatr. Neurol. *46*, 13–23.
2. Bushby, K. (2009). Diagnosis and management of the limb girdle muscular dystrophies. Pract. Neurol. *9*, 314–323.
3. Pegoraro, E., and Hoffman, E. (2000, updated 2012). Limb-Girdle Muscular Dystrophy Overview. In GeneReviews™ [Internet], Pagon RA, Bird TD, Dolan CR, et al., ed. (University of Washington, Seattle, WA, USA), 1993-. http://www.ncbi.nlm.nih.gov/books/NBK1408/
4. Minetti, C., Sotgia, F., Bruno, C., Scartezzini, P., Broda, P., Bado, M., Masetti, E., Mazzocco, M., Egeo, A., Donati, M.A., et al. (1998). Mutations in the caveolin-3 gene cause autosomal dominant limb-girdle muscular dystrophy. Nat. Genet. *18*, 365–368.

5. Richard, I., Broux, O., Allamand, V., Fougerousse, F., Chiannilkulchai, N., Bourg, N., Brenguier, L., Devaud, C., Pasturaud, P., Roudaut, C., et al. (1995). Mutations in the proteolytic enzyme calpain 3 cause limb-girdle muscular dystrophy type 2A. Cell *81*, 27–40.
6. Mercuri, E., and Muntoni, F. (2012). The ever-expanding spectrum of congenital muscular dystrophies. Ann. Neurol. *72*, 9–17.
7. American Association on Intellectual and Developmental Disabilities. (2010). Intellectual disability: definition, classification, and systems of supports (Washington, DC: American Association on Intellectual and Developmental Disabilities).
8. Kaufman, L., Ayub, M., and Vincent, J.B. (2010). The genetic basis of non-syndromic intellectual disability: a review. J Neurodev Disord *2*, 182–209.
9. van Bokhoven, H. (2011). Genetic and epigenetic networks in intellectual disabilities. Annu. Rev. Genet. *45*, 81–104.
10. Boycott, K.M., Parboosingh, J.S., Chodirker, B.N., Lowry, R.B., McLeod, D.R., Morris, J., Greenberg, C.R., Chudley, A.E., Bernier, F.P., Midgley, J., et al. (2008). Clinical genetics and the Hutterite population: a review of Mendelian disorders. Am. J. Med. Genet. A. *146A*, 1088–1098.
11. Hostetler, J.A. (1985). History and relevance of the Hutterite population for genetic studies. Am. J. Med. Genet. *22*, 453–462.
12. Abecasis, G.R., Cherny, S.S., Cookson, W.O., and Cardon, L.R. (2001). GRR: graphical representation of relationship errors. Bioinformatics *17*, 742–743.
13. O'Connell, J.R., and Weeks, D.E. (1998). PedCheck: a program for identification of genotype incompatibilities in linkage analysis. Am. J. Hum. Genet. *63*, 259–266.
14. Abecasis, G.R., Cherny, S.S., Cookson, W.O., and Cardon, L.R. (2002). Merlin—rapid analysis of dense genetic maps using sparse gene flow trees. Nat. Genet. *30*, 97–101.
15. Gudbjartsson, D.F., Jonasson, K., Frigge, M.L., and Kong, A. (2000). Allegro, a new computer program for multipoint linkage analysis. Nat. Genet. *25*, 12–13.
16. Thiele, H., and Nürnberg, P. (2005). HaploPainter: a tool for drawing pedigrees with complex haplotypes. Bioinformatics *21*, 1730–1732.
17. Corpet, F. (1988). Multiple sequence alignment with hierarchical clustering. Nucleic Acids Res. *16*, 10881–10890.
18. Frosk, P., Weiler, T., Nylen, E., Sudha, T., Greenberg, C.R., Morgan, K., Fujiwara, T.M., and Wrogemann, K. (2002). Limb-girdle muscular dystrophy type 2H associated with mutation in TRIM32, a putative E3-ubiquitin-ligase gene. Am. J. Hum. Genet. *70*, 663–672.
19. Frosk, P., Greenberg, C.R., Tennese, A.A., Lamont, R., Nylen, E., Hirst, C., Frappier, D., Roslin, N.M., Zaik, M., Bushby, K., et al. (2005). The most common mutation in FKRP causing limb girdle muscular dystrophy type 2I (LGMD2I) may have occurred only once and is present in Hutterites and other populations. Hum. Mutat. *25*, 38–44.
20. Kim, Y.G., Raunser, S., Munger, C., Wagner, J., Song, Y.L., Cygler, M., Walz, T., Oh, B.H., and Sacher, M. (2006). The architecture of the multisubunit TRAPP I complex suggests a model for vesicle tethering. Cell *127*, 817–830.
21. Sacher, M., Jiang, Y., Barrowman, J., Scarpa, A., Burston, J., Zhang, L., Schieltz, D., Yates, J.R., 3rd, Abeliovich, H., and Ferro-Novick, S. (1998). TRAPP, a highly conserved novel complex on the cis-Golgi that mediates vesicle docking and fusion. EMBO J. *17*, 2494–2503.
22. Scrivens, P.J., Noueihed, B., Shahrzad, N., Hul, S., Brunet, S., and Sacher, M. (2011). C4orf41 and TTC-15 are mammalian TRAPP components with a role at an early stage in ER-to-Golgi trafficking. Mol. Biol. Cell *22*, 2083–2093.
23. Sadler, K.C., Amsterdam, A., Soroka, C., Boyer, J., and Hopkins, N. (2005). A genetic screen in zebrafish identifies the mutants vps18, nf2 and foie gras as models of liver disease. Development *132*, 3561–3572.
24. Gross, J.M., Perkins, B.D., Amsterdam, A., Egaña, A., Darland, T., Matsui, J.I., Sciascia, S., Hopkins, N., and Dowling, J.E. (2005). Identification of zebrafish insertional mutants with defects in visual system development and function. Genetics *170*, 245–261.
25. Wendler, F., Gillingham, A.K., Sinka, R., Rosa-Ferreira, C., Gordon, D.E., Franch-Marro, X., Peden, A.A., Vincent, J.P., and Munro, S. (2010). A genome-wide RNA interference screen identifies two novel components of the metazoan secretory pathway. EMBO J. *29*, 304–314.
26. Bergmann, J.E., and Singer, S.J. (1983). Immunoelectron microscopic studies of the intracellular transport of the membrane glycoprotein (G) of vesicular stomatitis virus in infected Chinese hamster ovary cells. J. Cell Biol. *97*, 1777–1787.
27. Hirschberg, K., Miller, C.M., Ellenberg, J., Presley, J.F., Siggia, E.D., Phair, R.D., and Lippincott-Schwartz, J. (1998). Kinetic analysis of secretory protein traffic and characterization of golgi to plasma membrane transport intermediates in living cells. J. Cell Biol. *143*, 1485–1503.
28. Humphries, W.H., 4th, Szymanski, C.J., and Payne, C.K. (2011). Endo-lysosomal vesicles positive for Rab7 and LAMP1 are terminal vesicles for the transport of dextran. PLoS ONE *6*, e26626.
29. Bassik, M.C., Kampmann, M., Lebbink, R.J., Wang, S., Hein, M.Y., Poser, I., Weibezahn, J., Horlbeck, M.A., Chen, S., Mann, M., et al. (2013). A systematic mammalian genetic interaction map reveals pathways underlying ricin susceptibility. Cell *152*, 909–922.
30. Moreau, D., Kumar, P., Wang, S.C., Chaumet, A., Chew, S.Y., Chevalley, H., and Bard, F. (2011). Genome-wide RNAi screens identify genes required for Ricin and PE intoxications. Dev. Cell *21*, 231–244.
31. Ganley, I.G., Carroll, K., Bittova, L., and Pfeffer, S. (2004). Rab9 GTPase regulates late endosome size and requires effector interaction for its stability. Mol. Biol. Cell *15*, 5420–5430.
32. Lebrand, C., Corti, M., Goodson, H., Cosson, P., Cavalli, V., Mayran, N., Fauré, J., and Gruenberg, J. (2002). Late endosome motility depends on lipids via the small GTPase Rab7. EMBO J. *21*, 1289–1300.
33. Gedeon, A.K., Colley, A., Jamieson, R., Thompson, E.M., Rogers, J., Sillence, D., Tiller, G.E., Mulley, J.C., and Gécz, J. (1999). Identification of the gene (SEDL) causing X-linked spondyloepiphyseal dysplasia tarda. Nat. Genet. *22*, 400–404.
34. Mochida, G.H., Mahajnah, M., Hill, A.D., Basel-Vanagaite, L., Gleason, D., Hill, R.S., Bodell, A., Crosier, M., Straussberg, R., and Walsh, C.A. (2009). A truncating mutation of TRAPPC9 is associated with autosomal-recessive intellectual disability and postnatal microcephaly. Am. J. Hum. Genet. *85*, 897–902.
35. Mir, A., Kaufman, L., Noor, A., Motazacker, M.M., Jamil, T., Azam, M., Kahrizi, K., Rafiq, M.A., Weksberg, R., Nasr, T., et al. (2009). Identification of mutations in TRAPPC9, which encodes the NIK- and IKK-beta-binding protein, in nonsyndromic autosomal-recessive mental retardation. Am. J. Hum. Genet. *85*, 909–915.

36. Zong, M., Wu, X.G., Chan, C.W., Choi, M.Y., Chan, H.C., Tanner, J.A., and Yu, S. (2011). The adaptor function of TRAPPC2 in mammalian TRAPPs explains TRAPPC2-associated SEDT and TRAPPC9-associated congenital intellectual disability. PLoS ONE *6*, e23350.
37. Nishino, I., Fu, J., Tanji, K., Yamada, T., Shimojo, S., Koori, T., Mora, M., Riggs, J.E., Oh, S.J., Koga, Y., et al. (2000). Primary LAMP-2 deficiency causes X-linked vacuolar cardiomyopathy and myopathy (Danon disease). Nature *406*, 906–910.
38. Boucek, D., Jirikowic, J., and Taylor, M. (2011). Natural history of Danon disease. Genet. Med. *13*, 563–568.
39. Prall, F.R., Drack, A., Taylor, M., Ku, L., Olson, J.L., Gregory, D., Mestroni, L., and Mandava, N. (2006). Ophthalmic manifestations of Danon disease. Ophthalmology *113*, 1010–1013.

American Journal of Human Genetics, Volume *93*

Supplemental Information

Recessive *TRAPPC11* Mutations Cause a Disease Spectrum of Limb Girdle Muscular Dystrophy and Myopathy with Movement Disorder and and Intellectual Disability

Nina Bögershausen, Nassim Shahrzad, Jessica X. Chong, Jürgen-Christoph von Kleist-Retzow, Daniela Stanga, Yun Li, Francois P. Bernier, Catrina M. Loucks, Radu Wirth, Eric G. Puffenberger, Robert A Hegele, Julia Schreml, Gabriel Lapointe, Katharina Keupp, Christopher L. Brett, Rebecca Anderson, Andreas Hahn, A. Micheil Innes, Oksana Suchowersky, Marilyn B. Mets, Gudrun Nürnberg, D. Ross McLeod, Holger Thiele, Darrel Waggoner, Janine Altmüller, Kym M. Boycott, Benedikt Schoser, Peter Nürnberg, Carole Ober, Raoul Heller, Jillian S. Parboosingh, Bernd Wollnik, Michael Sacher, and Ryan E. Lamont

Supplemental Inventory

Supplemental Figures and Tables

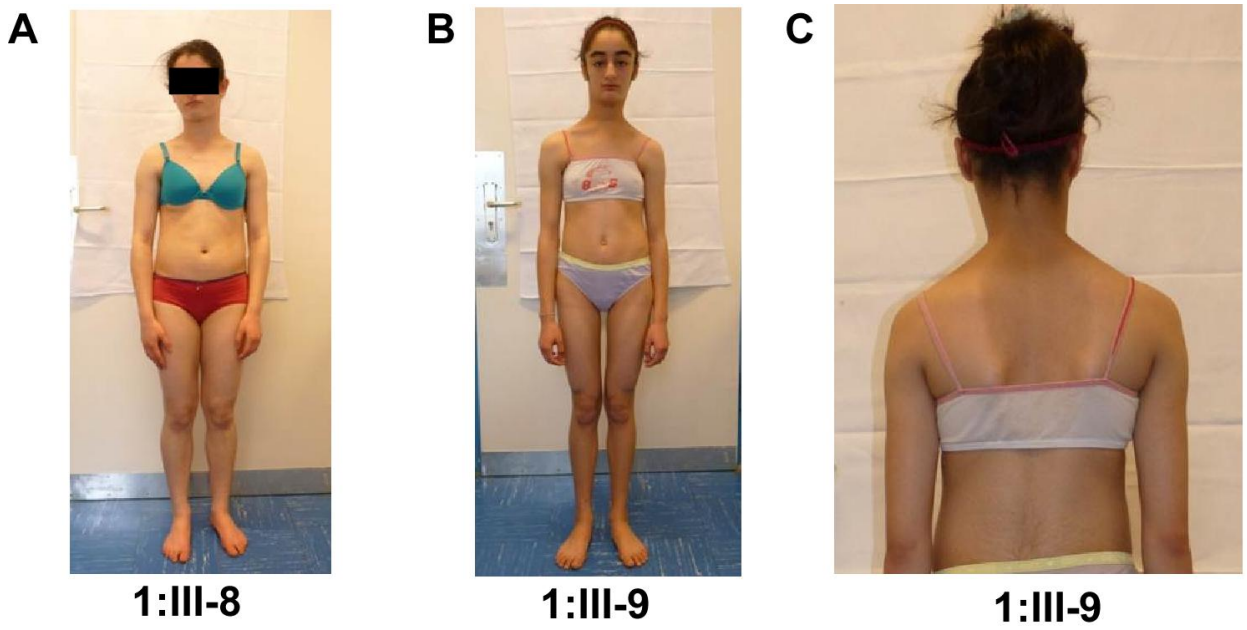
A
B
C
1:III-8
1:III-9
1:III-9

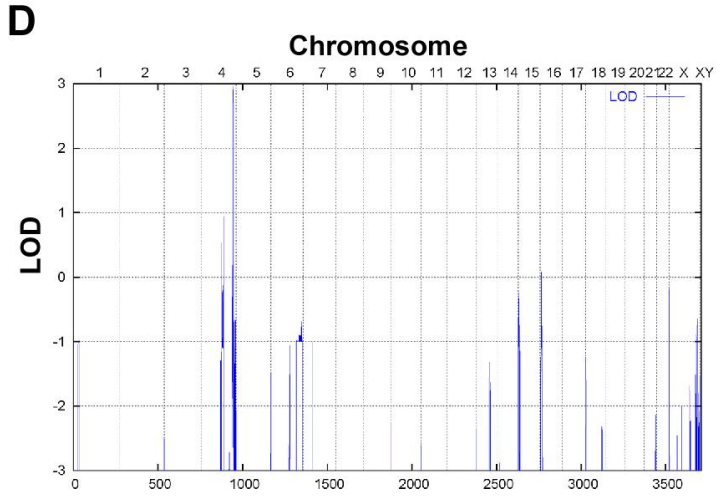
D
Chromosome
1 2 3 4 5 6 7 8 9 10 11 12 13 14 15 16 17 18 19 20 21 22 X XY
LOD
3
2
1
0
-1
-2
-3
0 500 1000 1500 2000 2500 3000 3500

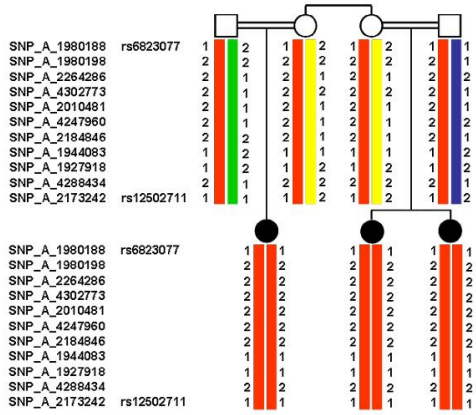
E
SNP_A_1980188 rs6823077
SNP_A_1980198
SNP_A_2264286
SNP_A_4302773
SNP_A_2010481
SNP_A_4247960
SNP_A_2184846
SNP_A_1944083
SNP_A_1927918
SNP_A_4288434
SNP_A_2173242 rs12502711

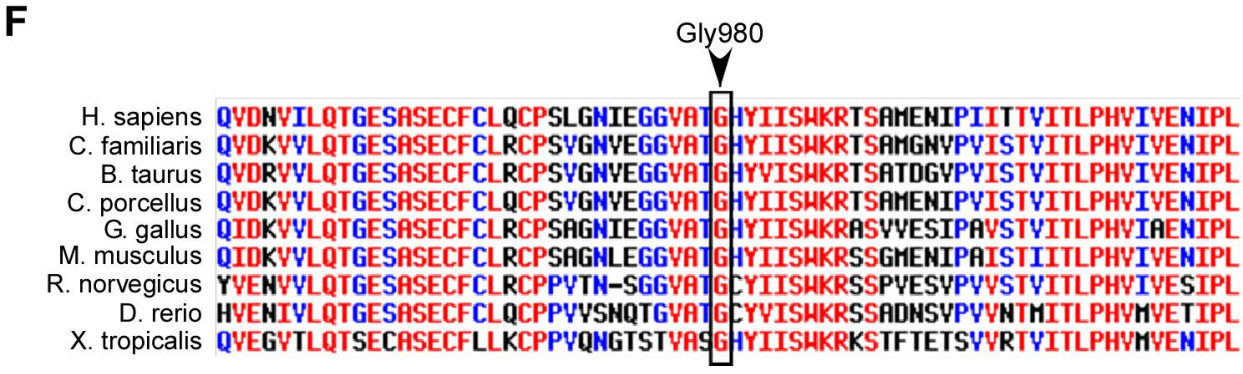
F
Gly980
H. sapiens QVDNVILQTGESASECFCLQCPSLGNIEGGVATGHYIISWKRTSAMENIPIITTVITLPHVIVENIPL
C. familiaris QVDKVVLQTGESASECFCLRCPSVGNVEGGVATGHYIISWKRTSAMGNVPVISTVITLPHVIVENIPL
B. taurus QVDRVVLQTGESASECFCLRCPSVGNVEGGVATGHYVISWKRTSATDGVPVISTVITLPHVIVENIPL
C. porcellus QVDKVVLQTGESASECFCLQCPSVGNVEGGVATGHYIISWKRTSAMENIPVISTVITLPHVIVENIPL
G. gallus QIDKVVLQTGESASECFCLRCPSAGNIEGGVATGHYIISWKRASVVESIPAVSTVITLPHVIAENIPL
M. musculus QIDKVVLQTGESASECFCLRCPSAGNLEGGVATGHYIISWKRSSGMENIPAISTIITLPHVIVENIPL
R. norvegicus YVENVVLQTGESASECFCLRCPPVTN-SGGVATGCYIISWKRSSPVESVPVVSTVITLPHVIVESIPL
D. rerio HVENIVLQTGESASECFCLQCPPVVSNQTGVATGCYVISWKRSSADNSVPVVNTMITLPHVMVETIPL
X. tropicalis QVEGVTLQTSECASECFLLKCPPVQNGTSTVASGHYIISWKRKSTFTETSVVRTVITLPHVMVENIPL

Figure S1. Photographs of Affected Individuals and Mapping Data of Family 1

(A-C) Pictures of individuals III-8 and III-9 from family 1 at 20 and 16 years of age, respectively; note the myopathic facial expression, and slight scapular winging in individual III-9.

(D) Genome-wide graphical view of LOD score calculations from family 1 indicating a single linked region on chromosome 4q35.1.

(E) Haplotypes of family 1 for the linked region on chromosome 4 show homozygosity in all three affected individuals whereas the parents are heterozygous for the disease haplotype. Displayed SNPs are exemplary for the original data set.

(F) C11 multiple species alignment in the region of the p.Gly980Arg substitution using Mutalin[18]. Residues in red are highly conserved and residues in blue are moderately conserved.

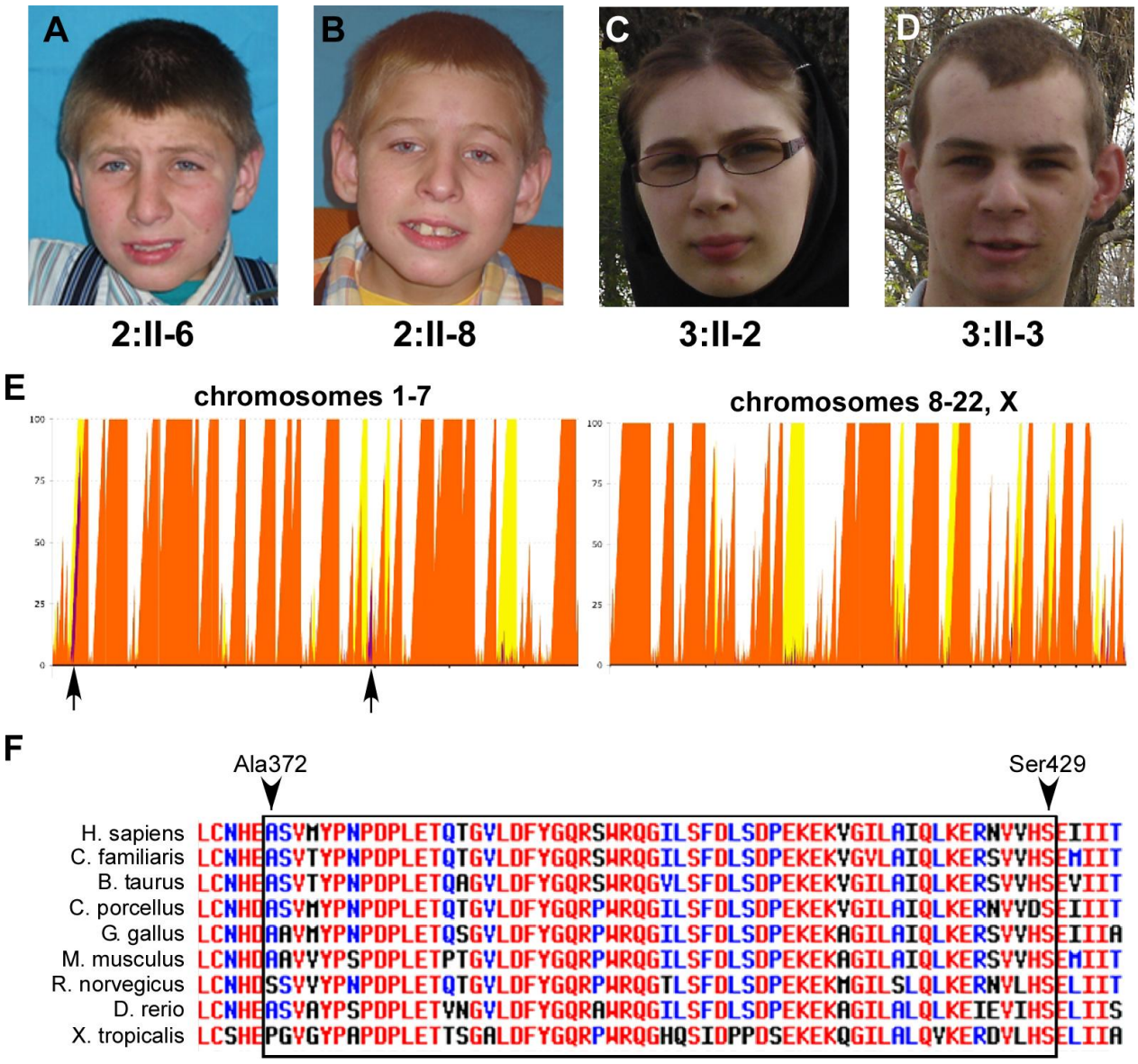

Figure S2. Photographs of Affected Individuals and Mapping Data of Families 2 and 3

(A and B) Facial features of individuals II-6 and II-8 from family 2.

(C and D) Facial features of individuals II-2 and II-3 from family 3.

(E) SNP genotyping using the Affymetrix 10K microarray in two affected siblings and two unaffected siblings in family 2 identified two regions (indicated by arrows) where both affected siblings shared a block of homozygous SNPs that were not shared by the two unaffected siblings.

(F) C11 multiple species alignment in the region of the 58 amino acid in-frame deletion (p.Ala372_Ser429del) using Mutalin[18]. Residues in red are highly conserved and residues in blue are moderately conserved.

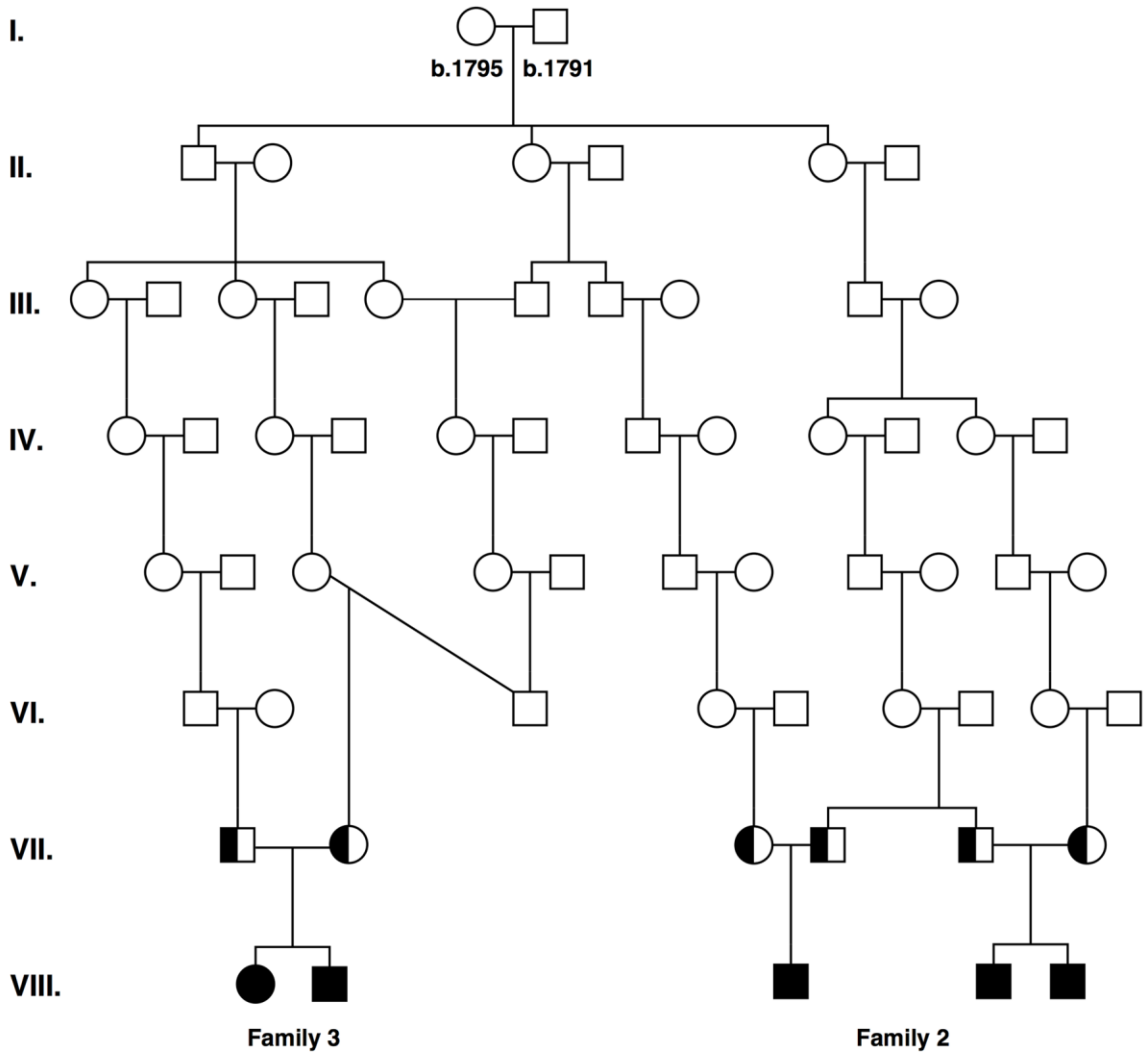

Figure S3. Extended Pedigree of the Hutterite Families

All five affected individuals can be traced back eight generations to their most recent common ancestors, a couple born in the 1790s, neither of whom is a founder of the Hutterite pedigree. Black-filled symbols are affected individuals in this study and half-filled symbols are heterozygous carrier parents.

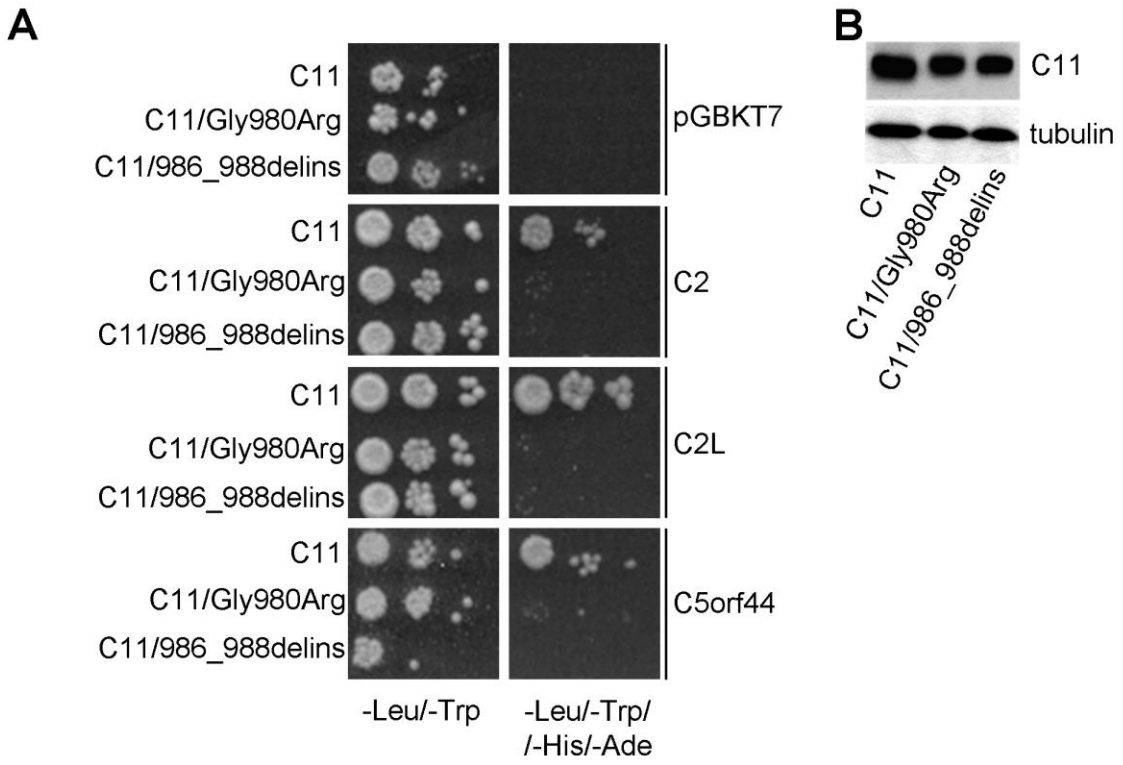

Figure S4. The p.Gly980Arg Substitution in TRAPPC11 Weakens Its Interactions with Several TRAPP Proteins

(A) The open reading frames for wild type C11, C11 p.Gly980Arg and C11 p.Trp986_Arg988delinsAlaGluAsp were cloned into pGADT7 and co-expressed in yeast cells with either an empty pGBKT7 vector or pGBKT7 containing other TRAPP components. Serial dilutions of the *S. cervisiae* cells spotted onto plates lacking either leucine and tryptophan, or leucine, tryptophan, histidine and adenine. Growth on the latter plates is a qualitative measure of the interaction between two proteins. Interactions with the TRAPP components C2, C2L and C5orf44 are compromised in the presence of the p.Gly980Arg substitution and in C11 p.Trp986_Arg988delinsAlaGluAsp.

(B) Lysates were prepared from the yeast cells containing C11 or one of the C11 mutants together with pGBKT7. Western blotting for the C11 protein (expressed as a fusion with the Gal4 activation domain and a myc epitope tag) using anti-myc IgG, or tubulin as a loading control. The results suggest that the compromised interactions are not due to reduced protein levels in the yeast cells

Table S1. Variants within Chromosome 4q35.1 Homozygous Region in Family 1

Position	Gene	Base	Protein	Depth	Freq.	Rs number
184170025	*WWC2*	G/A	+12_12	108	100	rs907357
184190233	*WWC2*	G/T	Ala773Pro	508	99	rs11941467
184243528	*CLDN24*	G/A	Leu10Ile	320	100	rs7688467
184570715	*RWDD4*	T/G	Ile124Leu	249	100	rs10015804
184618936	*TRAPPC11*	G/C	Gln933His	67	100	rs62617790
184622936	***TRAPPC11***	**G/A**	**Gly980Arg**	**121**	**100**	**--**
185012398	*ENPP6*	T/C	Ser419Gly	38	100	rs4479748
185074686	*ENPP6*	A/C	-21_21	40	100	rs13147555

Table S2. Genes within the Chromosome 4q34.3-q35.1 Candidate Region in Family 2

	GeneSymbol	Refseq	cds Start	cds End
	rs721684		177850523	
1	*7SK*		178102595	178102595
2	*NEIL3*	NM_018248	178231107	178283625
3	*AGA*	NM_000027	178352861	178363529
4	*AK094945*		178366132	178366132
5	*U7*		178502012	178502012
6	*LOC285501*		178649910	178649910
7	*Mir_544*		180349726	180349726
8	*LINC00290*		181985242	181985242
9	*AK056196*		182896308	182896308
10	*MGC45800*		183060158	183060158
11	*MIR1305*		183090445	183090445
12	*ODZ3*	NM_001080477	183245173	183721504
13	*U2*		183469811	183469811
14	*DCTD*	NM_001921	183812551	183836721
15	*FAM92A3*		183958817	183958817
16	*C4orf38*		184019137	184019740
17	*WWC2*	NM_024949	184020644	184236882
18	*U7*		184090500	184090500
19	*BX537950*		184154780	184154780

20	*CLDN22*	NM_001111319	184240708	184241371
21	*CLDN24*	NM_001185149	184242916	184243579
22	*CDKN2AIP*	NM_017632	184365950	184368580
23	*LOC389247*		184415889	184415889
24	*ING2*	NM_001564	184426348	184432105
25	*RWDD4*	NM_152682	184562588	184580105
26	*U6*		184574724	184574724
27	***TRAPPC11***	**NM_199053**	**184585020**	**184633775**
28	*U6*		184596755	184596755
29	*U6*		184627083	184627083
30	*STOX2*	NM_020225	184827943	184938437
31	*AK001394*		184940455	184940455
32	*ENPP6*	NM_153343	185012329	185138972
33	*LOC728175*		185262183	185262183
34	*AK126253*		185286340	185286340
35	*IRF2*	NM_002199	185309911	185350218
36	*CASP3*	NM_004346	185550425	185559607
37	*CCDC111*	NM_152683	185578294	185615933
38	*MLF1IP*	NM_024629	185616441	185655216
39	*ACSL1*	NM_001995	185678278	185724668
40	*SLED1*		185719450	185719450
41	*LOC731424*		185764449	185764449
42	*BC016366*		185765736	185765736
43	*MIR3945*		185772166	185772166
44	*LOC100506229*		185814153	185814153
45	*HELT*	NM_001029887	185940082	185941926
46	*BC043280*		185973049	185973049
47	*SLC25A4*	NM_001151	186064526	186068125
48	*KIAA1430*	NM_020827	186083951	186112350
49	*SNX25*	NM_031953	186168510	186284619
50	*LRP2BP*	NM_018409	186288333	186299340
51	*BC128459*		186298664	186298664
52	*ANKRD37*	NM_181726	186318077	186320931
53	*UFSP2*	NM_018359	186321545	186347022

54	*C4orf47*	NM_001114357	186350565	186370798
55	*CCDC110*	NM_152775	186379256	186392837
56	*PDLIM3*	NM_014476	186423447	186456588
57	*SORBS2*	NM_003603	186508780	186611725
	rs726466		186546056	

The region of identity-by-descent was flanked by the SNPs rs721684 and rs726466.

Table S3. Genotyping Results for *TRAPPC11* c.1287+5G>A in Hutterite Control Cohorts

Leut	Genotype			Total	Carrier frequency	Expected homozygous frequency
	G/G	G/A	A/A			
Dariusleut	176	14	0	190	0.071 (1/14)	1/793
Lehrerleut	190	0	0	190	0	0
Schmiedeleut	1335	112	0	1447	0.074 (1/13.5)	1/730

Table S4. Quantitative β-galactosidase Assay (Units of Activity)

	pGADT7	C2	C2L	C5orf44 (C13)
C11	0.44+/-0.09	8.64+/-1.68	27.5+/-4.65	53+/-4.32
C11/G980R	0.51+/-0.08	0.91+/-0.12	1.29+/-0.34	0.97+/-0.38
C11/WKR986-988AED	0.47+/-0.23	0.75+/-0.07	0.98+/-0.17	0.36+/-0.09

The yeast cells corresponding to Figure S4 were subjected to a quantitative β-galactosidase assay to measure the strength of interaction between the C11 proteins and the indicated TRAPP proteins. The assays were performed in triplicate and the units of activity are indicated along with the standard error of the mean (SEM).